



Published in final edited form as:

*Heart Rhythm*. 2021 February ; 18(2): 250–260. doi:10.1016/j.hrthm.2020.09.007.

## Calcium signaling consequences of RyR2 mutations associated with CPVT1 introduced via CRISPR/Cas9 gene editing in human-induced pluripotent stem cell–derived cardiomyocytes: Comparison of RyR2-R420Q, F2483I, and Q4201R

Xiao-Hua Zhang, PhD, Hua Wei, PhD, Yanli Xia, PhD, Martin Morad, PhD

Cardiac Signaling Center of University of South Carolina, Medical University of South Carolina, and Clemson University, Charleston, South Carolina

### Abstract

**BACKGROUND**—Human-induced pluripotent stem cell–derived cardiomyocytes (hiPSC-CMs) created from patients with catecholaminergic polymorphic ventricular tachycardia 1 (CPVT1) have been used to study CPVT1 arrhythmia.

**OBJECTIVE**—The purpose of this study was to evaluate the Ca<sup>2+</sup> signaling aberrancies and pharmacological sensitivities of 3 CRISPR/Cas9-introduced CPVT1 mutations located in different molecular domains of ryanodine receptor 2 (RyR2).

**METHODS**—CRISPR/Cas9-engineered hiPSC-CMs carrying RyR2 mutations—R420Q, Q4201R, and F2483I—were voltage clamped, and their electrophysiology, pharmacology, and Ca<sup>2+</sup> signaling phenotypes measured using total internal reflection fluorescence microscopy.

**RESULTS**—R420Q and Q4201R mutant hiPSC-CMs exhibit irregular, long-lasting, spatially wandering Ca<sup>2+</sup> sparks and aberrant Ca<sup>2+</sup> releases similar to F2483I unlike the wild-type myocytes. Large sarcoplasmic reticulum (SR) Ca<sup>2+</sup> leaks and smaller SR Ca<sup>2+</sup> contents were detected in cells expressing Q4201R and F2483I, but not R420Q. Fractional Ca<sup>2+</sup> release and calcium-induced calcium release gain were higher in Q4201R than in R420Q and F2483I hiPSC-CMs. JTV519 was equally effective in suppressing Ca<sup>2+</sup> sparks, waves, and SR Ca<sup>2+</sup> leaks in hiPSC-CMs derived from all 3 mutant lines. Flecainide and dantrolene similarly suppressed SR Ca<sup>2+</sup> leaks, but were less effective in decreasing spark frequency and durations.

**CONCLUSION**—CRISPR/Cas9 gene editing of hiPSCs provides a novel approach in studying CPVT1-associated RyR2 mutations and suggests that Ca<sup>2+</sup>-signaling aberrancies and drug sensitivities may vary depending on the mutation site.

### Graphical Abstract

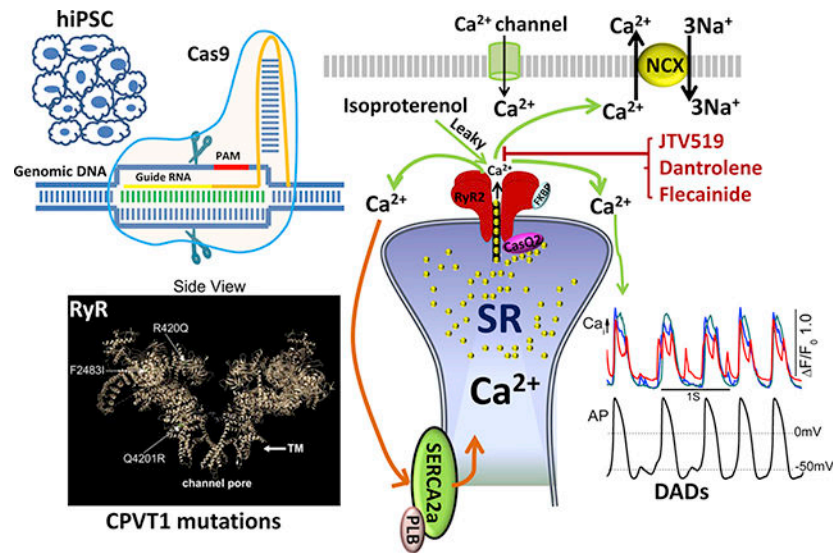
---

**Address reprint requests and correspondence:** Dr. Martin Morad, Cardiac Signaling Center of University of South Carolina, Medical University of South Carolina, and Clemson University, 68 President St, Bioengineering Building, Room 306, Charleston, SC 29403. moradm@musc.edu.

Appendix

Supplementary data

Supplementary data associated with this article can be found in the online version at <https://doi.org/10.1016/j.hrthm.2020.09.007>.



## Keywords

Ca<sup>2+</sup> sparks; CPVT1; CRISPR/Cas9; hiPSC-CMs; JTV519; RyR2

## Introduction

Cardiac excitation-contraction coupling is mediated by activation of the calcium-induced calcium release (CICR) mechanism that triggers Ca<sup>2+</sup> release from sarcoplasmic reticulum (SR) during each action potential.<sup>1</sup> Dysfunctions in Ca<sup>2+</sup> signaling may result in cardiac hypertrophy, failure, and arrhythmias.<sup>2-4</sup> Missense mutations in human ryanodine receptor 2 (RYR2) have been shown to associate with catecholaminergic polymorphic ventricular tachycardia 1 (CPVT1), a life-threatening arrhythmia.<sup>5</sup> Thus far, >150 missense mutations, spread all over the ~5000-amino acid RyR2 polypeptide, are identified to associate with CPVT1.<sup>6,7</sup> Functional consequences of CPVT1 mutations have been studied by heterologous expression of the recombinant mutants of RyR2 and knock-in mutation in mouse models.<sup>8,9</sup> These studies have led to proposals that CPVT1 pathology results either from phosphorylation-induced leakiness of the RyR2 channel<sup>10,11</sup> or from the Ca<sup>2+</sup> overload of SR.<sup>12</sup> Such aberrant Ca<sup>2+</sup> releases activate the Na/Ca exchanger to depolarize the myocytes, triggering early afterdepolarizations or delayed afterdepolarizations and arrhythmias.<sup>13,14</sup> Despite the insights gained from such studies, a systematic mutation-dependent comparison of Ca<sup>2+</sup>-signaling aberrancies of CPVT1 pathology in human cardiomyocytes has not been possible and is desirable.

The advent of hiPSCs<sup>15</sup> and CRISPR/Cas9 genome editing make it possible to carry out such comparisons using fibroblast-derived cardiomyocytes,<sup>16</sup> where point mutations associated with CPVT1 are introduced in wild-type (WT) human cardiomyocytes to quantify the Ca<sup>2+</sup> signaling aberrancies of different mutations and determine whether disease-associated mutations are causative or associative. We have already reported that CRISPR/Cas9 gene-edited human-induced pluripotent stem cell-derived cardiomyocytes (hiPSC-

CMs) carrying F2483I-RyR2 mutation exhibit aberrant Ca<sup>2+</sup> signaling properties indistinguishable from those recorded in patient-derived cells carrying F2483I mutation.<sup>17</sup> Therefore, we undertook detailed comparisons of Ca<sup>2+</sup> signaling and pharmacological profiles of 3 CPVT1 mutations, located in N-terminal R420Q, C-terminal Q4201R, and central-domain F2483I, to determine whether the molecular mechanism of CPVT1 pathology and its pharmacology depended on the RyR2 mutation site.

The data suggest that all 3 mutations express prolonged, wandering, and reigniting Ca<sup>2+</sup> sparks, but differ in their CICR gain, the Ca<sup>2+</sup> content of SR, its leakiness, and the sensitivity to antiarrhythmic drugs.

## Methods

### Maintenance of hiPSC lines

The hiPSC-K3 line was maintained in StemFlex Medium (Gibco, Thermo Fisher Scientific, Waltham, MA, US) and passaged with Versene as described previously.<sup>17,18</sup>

### CRISPR/Cas9 genome editing in hiPSCs

Two CPVT1 associated RyR2 mutations—R420Q and Q4201R—were introduced into the *RYR2* gene of WT hiPSCs by CRISPR/Cas9 gene editing, as described previously<sup>17</sup> (see Online Supplemental Materials).

### Differentiation of hiPSCs into functional cardiomyocytes

hiPSCs were differentiated into cardiomyocytes using protocols described previously.<sup>17,18</sup> Three to four weeks after spontaneous beating started, beating clusters were enzymatically (TrypLE Select Enzyme [10×], Gibco) dissociated into single cardiomyocytes for Ca<sup>2+</sup> signaling experiments. The same batch of differentiated cells was used for up to 3 months.

### Quantitative reverse transcription polymerase chain reaction(RT-PCR) and Western blot

Total RNAs and proteins of hiPSC-CMs were collected at day 45 after differentiation for analysis. For method details and primer selections, see Online Supplemental Materials.

### Measurements of Ca<sup>2+</sup> transients and sparks

Fluo-4AM (Invitrogen, Thermo Fisher Scientific, Waltham, MA, US)–incubated hiPSC-CMs were imaged using multi-color total internal reflection fluorescence (TIRF) microscopy. Ca<sup>2+</sup> sparks were recorded at 60–80 Hz with a depth of penetration of 110–150 nm. Sparks data were exported and analyzed with Leica LAS X (Leica Microsystems Inc, Wetzlar, Germany) and Con2i (custom developed by our lab) software as described previously.<sup>17</sup>

### Electrophysiology

All electrophysiological and Ca<sup>2+</sup> transient measurements were carried out simultaneously in whole-cell patch-clamped hiPSC-CMs at 32°C–35°C (see Online Supplemental Materials).

## SR Ca<sup>2+</sup> leak and load measurement

The SR Ca<sup>2+</sup> content and diastolic Ca<sup>2+</sup> leak of WT and mutant hiPSC-CMs were measured as described previously<sup>17</sup> (see Online Supplemental Materials).

## Statistical analysis

The results are presented as mean ± SEM. Comparative analysis was performed using 1-way analysis of variance followed by the Tukey test or Student *t* test. Significant differences are labeled with 1 (\**P* < .05) or 2 (\*\**P* < .01) asterisks.

## Results

### Creation of hiPSC lines harboring R420Q and Q4201R RyR2 mutations

We used CRISPR/Cas9 gene editing to introduce R420Q and Q4201R mutations into the *RYR2* gene of control hiPSCs, as described for F2483I,<sup>17</sup> where it was shown that heterozygous and homozygous F2483I mutants had similar arrhythmogenic profiles.<sup>17</sup> The molecular sites of these mutations are shown in the 4.2 Å resolution cryoelectron microgram image of the purified pig RyR2 (see Graphical Abstract). We created 2 new homozygous—Q4201R and R420Q—and 1 heterozygous—Q4201R—hiPSC lines and verified the mutations by restriction enzyme digest (Figure 1C) and sequencing of the polymerase chain reaction (PCR) product amplified from the target loci (Figures 1A and 1B). Quantitative RT-PCR analyses showed that the expression level of RyR2 messenger RNA in R420Q mutant hiPSC-CMs were essentially similar to those of WT cells, but Q4201R mutant hiPSC-CMs had significantly lower levels of RyR2 (Figure 1D). RyR2 protein expression levels of all 3 homozygous mutants were essentially the same as those of WT cells (Western blots in Figures 1E and 1F).

### Ca<sup>2+</sup> sparks in WT and mutant hiPSC-CMs

Ca<sup>2+</sup> signaling aberrancies of RyR2-CPVT1 mutations and their domain dependence were measured in 3 homozygous and 1 heterozygous mutations and compared with WT hiPSC-CMs. Figure 2 shows that spontaneously occurring Ca<sup>2+</sup> sparks in WT hiPSC-CMs were brief, igniting, and decaying rapidly, whereas sparks of the 3 homozygous mutant hiPSC-CMs were longer lasting with variable durations, often reigniting and setting off localized releases of Ca<sup>2+</sup> (Figures 2A–2D). Although these aberrancies were common to all 3 mutations, there were noticeable differences in spark durations and frequency among the 3 mutant lines. Figure 2E shows that the histogram of spark duration, measured at half-maximum amplitude, averaged 58.2 ± 2.1 ms in WT as compared with 113.0 ± 4.5 ms in R420Q-homozygous, 95.5 ± 3.4 ms in Q4201R-homozygous, 91.4 ± 3.7 ms in Q4201R-heterozygous, and 126.1 ± 4.9 ms in F2483I-homozygous mutants, consistent with the longer mean open time of mutant RyR2s. Despite the significantly increased spark durations, the frequency of the occurrence of spontaneously triggered sparks did not vary significantly among the mutant lines compared with WT (Figure 2F). The mean spark frequency of the R420Q mutant was consistently lower, especially when compared with the F2483I mutant (Figure 2F).

Figure 3 shows total internal reflection fluorescence images of spark evolution (indicated by an asterisk in Figure 2) in WT and the 3 homozygous mutants. The igniting and decaying times of the sparks from F2483I and R420Q hiPSC-CMs were much longer than those from WT or Q4201R cells. Taken together, our results indicated that all 3 mutants exhibited prolonged  $\text{Ca}^{2+}$  release times.

### SR $\text{Ca}^{2+}$ leak and content in mutant hiPSC-CMs

To check whether the gene-edited RyR2 mutations had altered SR function, we quantified their caffeine-triggered  $\text{Ca}^{2+}$  store and their diastolic  $\text{Ca}^{2+}$  leak by application of a cocktail containing 1 mM tetracaine in zero  $\text{Ca}^{2+}$  and  $\text{Na}^+$  solutions.<sup>17</sup> Figures 4A–4D show representative  $\text{Ca}^{2+}$  signals comparing the responses of R420Q, Q4201R, and F2483I homozygous myocytes with those of WT myocytes to application of the “tetracaine cocktail” followed by caffeine. The SR  $\text{Ca}^{2+}$  leak was significantly larger in F2483I and Q4201R homozygous hiPSC-CMs than in WT cells or a small leak of R420Q cells (Figure 4E). Consistent with the SR leak levels, the SR  $\text{Ca}^{2+}$  content of Q4201R and F2483I hiPSC-CMs were smaller than that of WT cells (Figure 4F), confirming that the larger diastolic leak results in smaller SR  $\text{Ca}^{2+}$  content.

### L-type $\text{Ca}^{2+}$ current ( $I_{\text{Ca}}$ ), fractional $\text{Ca}^{2+}$ release, and CICR gain

To determine the fractional  $\text{Ca}^{2+}$  release and CICR gain,  $I_{\text{Ca}}$  and its triggered  $\text{Ca}^{2+}$  transient were measured in cells dialyzed with 0.1 mM Fluo-4 pentapotassium salt while the SR content was determined by applying 5 mM caffeine (see Methods). Figures 5A–5D show representative traces of  $I_{\text{Ca}}$  and  $I_{\text{Ca}}$ -induced  $\text{Ca}^{2+}$  release,  $I_{\text{Ca}}$  tail currents (activated by repolarization from +80 to –50 mV) and their triggered  $\text{Ca}^{2+}$  transients, caffeine-triggered  $\text{Ca}^{2+}$  release, and  $\text{Na}^+/\text{Ca}^{2+}$  exchange current in WT and mutant myocytes.  $I_{\text{Ca}}$  densities from WT and the 3 mutant hiPSC-CMs averaged between 6.4 and 9.2 pA/pF, and the accompanying  $\text{Ca}^{2+}$  transients averaged from 0.96 to 1.8 pA/pF. The differences in  $I_{\text{Ca}}$  densities were not statistically significant between WT and mutant hiPSC-CMs (Figure 5E), but  $I_{\text{Ca}}$ -induced  $\text{Ca}^{2+}$  release in Q4201R heterozygote was significantly higher than that in F2483I and R420Q mutants, resulting in higher fractional  $\text{Ca}^{2+}$  release and CICR gains in Q4201R than in F2483I and R420Q myocytes (Figure 5F).

### Pharmacological sensitivity of the mutant lines

**Adrenergic enhancement of  $\text{Ca}^{2+}$  release**—Figure 6 shows the effectiveness of 500 nM isoprenaline in enhancing  $I_{\text{Ca}}$  and aberrant  $\text{Ca}^{2+}$  releases in WT and mutant hiPSC-CMs. As expected, adrenergic stimulation enhanced aberrant  $\text{Ca}^{2+}$  releases in >30% of the mutant cells.

**$\text{Ca}^{2+}$  sparks**—Since all 3 homozygous mutants had irregular long-lasting and reigniting sparks as compared with WT cells, we examined the effectiveness of JTV519, flecainide, and dantrolene (drugs reported to inhibit RyR2<sup>19–21</sup>) in altering the morphology and frequency of spontaneously occurring  $\text{Ca}^{2+}$  sparks. Figure 7 shows that 2  $\mu\text{M}$  JTV519, a 1,4-benzothiazepine derivative,<sup>20</sup> significantly shortened the spark duration and decreased the spark frequency in all 3 homozygous mutants. JTV519 also consistently suppressed the frequency and duration of sparks in the Q4201R heterozygous mutant (Online Supplemental

Figure 1). Flecainide decreased the spark frequency in all 3 mutants but had little effect on spark duration even in the Q4201R heterozygous mutant (Figures 7B, 7E, and 7H and Online Supplemental Figure 1). Dantrolene, is an inhibitor of RyR1 and used in treating malignant hyperthermia, also decreased the spark frequency in R420Q and F2483I-RyR2 mutants, consistent with its suppression of CPVT1 in a mouse model and CPVT1 patient-derived hiPSC-CMs,<sup>21,22</sup> but had little effect on spark characteristics of the Q4201R mutant. Dantrolene was less effective than JTV519 in shortening the spark duration (Figures 7C and 7I).

Spontaneously beating mutant hiPSC-CMs often showed aberrant local Ca<sup>2+</sup> transients, occurring in between the regular beats especially in Q4201R cells (Online Supplemental Figure 2), that were suppressed by 2 μM JTV519 in 88% of R420Q (22 of 25), 87% of Q4201R (13 of 15), and 79% of F2483I (11 of 14) mutant cells (Figure 8). JTV519 also abolished such aberrant Ca<sup>2+</sup> releases in 91% of heterozygous Q4201R mutant cells (10 of 11) (Online Supplemental Figure 1). Ten micromolar dantrolene was less effective than JTV519, suppressing only 27% (4 of 15) of aberrant focal Ca<sup>2+</sup> releases in R420Q, 40% (4 of 10) in Q4201R, and 22% (2 of 9) in F2483I cells. Flecainide (5 μM) was also effective in suppressing focal Ca<sup>2+</sup> releases but only in 44% of R420Q (4 of 9), 55% of Q4201R (6 of 11), and 38% of F2483I (5 of 13) cells. The effects of all 3 drugs were reversible, allowing serial comparison of the drugs on the same cell (Figure 8). Our results suggest that JTV519 is equally effective in suppressing Ca<sup>2+</sup> releases in all 3 mutants. The antiarrhythmic effectiveness of the 3 drugs was as follows: JTV519>flecainide≈dantrolene.

**SR Ca<sup>2+</sup> leak and load**—Since hiPSC-CMs of WT and the 3 homozygous mutants showed different levels of SR Ca<sup>2+</sup> leaks (Figure 4), we examined whether the 3 drugs preferentially suppressed the SR Ca<sup>2+</sup> leak and restored the SR Ca<sup>2+</sup> content. Online Supplemental Figure 3 shows that JTV519, dantrolene, and flecainide significantly, but to different extent, suppressed the Ca<sup>2+</sup> leak of all 3 mutants. JTV519 was especially effective on the F2483I mutant, suppressing the leak by ~65% (Online Supplemental Figure 3A) and restoring the SR Ca<sup>2+</sup> content (Online Supplemental Figure 3B). Similarly, the JTV519 suppression of the SR leak in R420Q or Q4201R cells was accompanied by recovery of the Ca<sup>2+</sup> content of SR. Flecainide also suppressed the Ca<sup>2+</sup> leak in all 3 lines, but its effect was somewhat weaker. In contrast, dantrolene was more effective in suppressing the SR Ca<sup>2+</sup> leak and the recovery of SR Ca<sup>2+</sup> load more effectively in Q4201R than in R420Q and F2483I hiPSC-CMs. These findings suggest that different mutant lines show different drug sensitivities, but more extensive dose-response relation is required to determine the specificity and effectiveness of the drugs.

## Discussion

This is the first comparative report of creating 3 CRISPR/Cas9 gene-edited CPVT1-RyR2 mutations in hiPSC-CMs, where electrophysiological and Ca<sup>2+</sup> imaging consequences of 3 point mutations in N, central, and C terminals of RyR2 are examined and their pharmacological sensitivities determined. We found that hiPSC-CMs from all 3 mutants exhibited long-lasting Ca<sup>2+</sup> sparks that often reignited and spatially wandered, causing variable degrees of the SR Ca<sup>2+</sup> leak. Only moderate differences in the drug sensitivities of



the 3 mutants were found. JTV519 was effective in suppressing aberrant  $\text{Ca}^{2+}$  sparks and releases, but showed no site-dependent mutation specificity, while dantrolene and flecainide effects, though mutation dependent, were variable and moderate compared with JTV519.

### Creation and selection of CRISPR/Cas9 gene-edited mutations

The 3 CPVT1 mutation lines were created from the same hiPSC-K3 line,<sup>23</sup> not only to have lines with the same genetic background but also to represent the 3 domains of RyR2 protein. To confirm the reliability of the CRISPR approach, we chose point mutations that had been either introduced in mouse models or CPVT1 patient-derived hiPSC-CMs that expressed them.<sup>16,24,25</sup> We used protospacer adjacent motif (PAM) mutations in single-stranded oligo donor nucleotide (ssODNs) to improve homology-directed repair (HDR) accuracy<sup>26</sup> and introduce other mutations that created new restriction enzyme sites for restriction fragment length polymorphisms (RFLP) analysis.

Although CPVT1 is expressed as a heterozygous mutation in patients, we were more successful in creating the homozygous mutation. We felt that the homozygous mutation clones may better represent the pathology of CPVT1 in in vitro cell models, because the heterotetrameric structure of RyR2 may minimize the expression of  $\text{Ca}^{2+}$  signaling aberrancies. Nevertheless, we succeeded in obtaining heterozygous clones of Q4201R (Figure 1) as well as F2483I<sup>17</sup> and found no obvious differences in their  $\text{Ca}^{2+}$  signaling phenotype regardless of whether only 1 allele or both alleles were mutated.

### Electrophysiological and $\text{Ca}^{2+}$ signaling consequences of the site-specific RyR2 mutations

hiPSC-CMs from all 3 mutants showed prolonged and wandering sparks interspersed with aberrant focal  $\text{Ca}^{2+}$  releases.<sup>18,19</sup> Although there were significant differences in the spark durations between WT and mutants, there were only some differences in spark occurrence frequencies between F2483I and R420Q (Figure 2). There were, however, significant differences in the magnitude of the  $\text{Ca}^{2+}$  leak or SR  $\text{Ca}^{2+}$  content among the mutants. The SR leak was larger and the SR content was smaller in F2483I and Q4201R mutants than in control or the R420Q mutant. The higher fractional  $\text{Ca}^{2+}$  releases and CICR gain of Q4201R mutation may be caused by the higher occurrence of  $\text{Ca}^{2+}$  waves and larger SR  $\text{Ca}^{2+}$  leaks. In contrast, the lower spark frequency may counteract the prolonged spark duration in R420Q mutation and result in only moderate SR leaks. The higher spark frequency, longer spark duration, and large leaks of the F2783I mutant may be caused by the proximity of this site to the FK506-binding protein (FKBP) binding site, causing the dissociation of FKBP from RyR2 and producing significantly larger leaks.

### Pharmacological and pathophysiological implications

**hiPSC-CMs as a platform for  $\text{Ca}^{2+}$  signaling pathology**—Although hiPSC-CMs have been used as in vitro models of human inherited cardiac pathologies, considerable controversy still exists as to their appropriateness for pathophysiological studies. Clearly, advantages include human cell sources of the same genetic background that are preferable to genetically engineered mice or recombinant human embryonic kidney (HEK) cell models. Nevertheless, there are developmental aspects of hiPSC-CM maturation, such as lack of T-tubular network, the polygonal-flat cellular shapes, disorganized sarcomeres, rhythmic

automaticity, and heterogeneity of cell cultures, expressing atrial, ventricular, and nodal action potentials, suggesting that hiPSC-CMs may represent fetal rather than adult cardiomyocytes. Our recent review systematically compares the functional aspects of Ca<sup>2+</sup> signaling of hiPSC-CMs with those of native mammalian cardiomyocytes and concludes that despite quantitative differences, the qualitative aspects of Ca<sup>2+</sup> signaling are extremely similar to those of adult cardiomyocytes.<sup>27</sup>

In the present study, the development of adult-type sarcomere structure and T-tubular network do not appear to play a major functional role in RyR2 Ca<sup>2+</sup> signaling, making it possible to use hiPSC-CMs as an appropriate platform for aberrancies associated with missense mutations of RyR2. We have identified significant differences between WT and mutant Ca<sup>2+</sup> sparks characteristics, SR Ca<sup>2+</sup> leaks and loads, and the rate of occurrence of aberrant focal Ca<sup>2+</sup> releases. Nevertheless, we have found that 5%–10% WT hiPSC-CMs also show age and culture-dependent arrhythmogenic phenotypes and hope that efforts to mature hiPSC-CMs will further improve their reliability as pathophysiological models.

**Pharmacological specificity**—Three drugs, JTV519, dantrolene, and flecainide, known for targeting RyR2 showed preferential RyR2 mutation site sensitivity. Dantrolene, reported to bind to RyR2 N-terminus amino acids 601–620<sup>28,29</sup> that rescues the arrhythmogenic phenotype of S406L RyR2 in patient-derived hiPSC-CMs<sup>21</sup> and being antiarrhythmic in human CPVT1-associated RyR2 R2474S/+ knock-in mouse model,<sup>22</sup> was less effective than JTV519 in suppressing Ca<sup>2+</sup> sparks and aberrant Ca<sup>2+</sup> releases in all 3 mutants. Nevertheless, dantrolene was more effective in suppressing the SR leak (Online Supplemental Figure 3) and aberrant Ca<sup>2+</sup> releases (Figure 8) in the Q4201R mutant than in the other 2 mutants, even though its effects on the Ca<sup>2+</sup> spark of Q4201R cells were less clear. Although this finding appears inconsistent with the idea that spontaneous Ca<sup>2+</sup> sparks play a dominant role in the SR Ca<sup>2+</sup> leak, we note that Ca<sup>2+</sup> sparks are not the only pathway that mediates the SR leak. Spark-independent RyR openings as well as RyR-independent pathway have been reported to contribute to SR leaks.<sup>30</sup> Our finding that dantrolene was more effective in suppressing the SR Ca<sup>2+</sup> leak and recovery of the Ca<sup>2+</sup> load of SR without affecting the Ca<sup>2+</sup> sparks of Q4201R mutant myocytes suggests that dantrolene may be suppressing the non-Ca<sup>2+</sup> sparks-mediated SR leak of the Q4201R mutant. The possibility that different mechanisms may contribute to SR Ca<sup>2+</sup> leaks among the various mutants has not been fully tested, but should be considered in future studies. Flecainide has been reported to abolish Ca<sup>2+</sup> abnormalities in 33% of L4115F, 30% of V4653F, and 52% of exon 3 deletion RyR2 mutations in hiPSC-CMs from patients with CPVT.<sup>31</sup> In our study, flecainide consistently suppressed the spark frequency in all 3 mutants without affecting the spark duration and moderately suppressed the aberrant Ca<sup>2+</sup> releases in 44% of R420Q, 55% of Q4201R, and 38% in F2483I (Figure 8). JTV519, though effective in suppressing the spark frequency and aberrant focal releases in all 3 mutants, showed little mutation site specificity (Figure 7). The higher efficacy of JTV519, as compared with flecainide or dantrolene, may be related to its proposed interaction with the FKBP binding site of RyR2. The specificity of these drugs in suppressing the aberrant Ca<sup>2+</sup> releases is weakened by the finding that the drugs also suppressed the regularly occurring beats.



## Study limitations

The structural and biophysical maturity of hiPSC-CMs as models for pathophysiological studies must be carefully considered. A small population of WT cells showed arrhythmogenic behavior, likely related to the immaturity of hiPSC-CMs that may be alleviated by the availability of more mature hiPSC-CMs. Detailed drug dose-response studies may also provide better insights into the mutation site specificity of drugs and determine their sensitivities for control vs diseased tissues.

## Conclusion

We have created CPVT1-associated mutations in 3 domains of RyR2 using CRISPR/Cas9 gene editing in hiPSC-CMs. Our results demonstrated that F2483I, R420Q, and Q4201R CPVT1 mutants express variable Ca<sup>2+</sup> signaling phenotype and pharmacological sensitivity. It is likely that as the pharmacological profiles of more mutants are studied, the therapy of CPVT1 pathology will be moving into the realm of personalized medicine with mutation-specific pharmacotherapy.

## Supplementary Material

Refer to Web version on PubMed Central for supplementary material.

## Acknowledgments

We thank N. Yamaguchi, PhD for supervising the CRISPR/Cas9 experiments. Part of the wild-type and F2483I-homozygous sparks data were previously published in *Cell Calcium*.

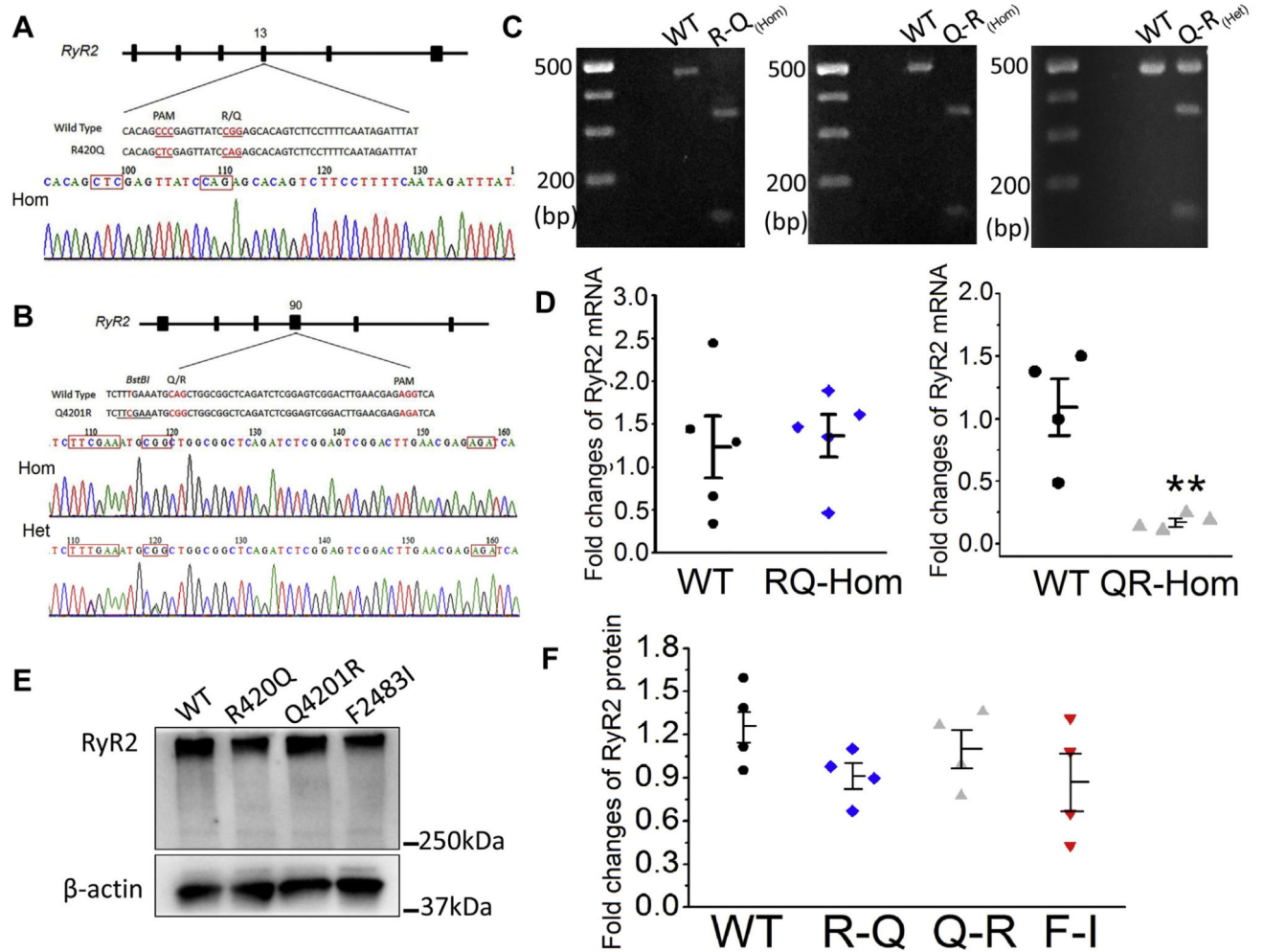
Sources of funding: The study was supported by the National Institutes of Health grant 1R56HL147054-01, and Jennifer Friedman Hillis Family Foundation Inc. Disclosures: The authors have no conflicts of interest to disclose.

## References

1. Nabauer M, Callewaert G, Cleemann L, Morad M. Regulation of calcium release is gated by calcium current, not gating charge, in cardiac myocytes. *Science* 1989; 244:800–803. [PubMed: 2543067]
2. Knollmann BC, Knollmann-Ritschel BE, Weissman NJ, Jones LR, Morad M. Remodelling of ionic currents in hypertrophied and failing hearts of transgenic mice overexpressing calsequestrin. *J Physiol* 2000;525:483–498. [PubMed: 10835049]
3. Zhang XH, Morad M. Calcium signaling in human stem cell-derived cardiomyocytes: evidence from normal subjects and CPVT afflicted patients. *Cell Calcium* 2016;59:98–107. [PubMed: 26725479]
4. Venetucci L, Denegri M, Napolitano C, Priori SG. Inherited calcium channelopathies in the pathophysiology of arrhythmias. *Nat Rev Cardiol* 2012; 9:561–575. [PubMed: 22733215]
5. Priori SG, Napolitano C, Tiso N, et al. Mutations in the cardiac ryanodine receptor gene (hRyR2) underlie catecholaminergic polymorphic ventricular tachycardia. *Circulation* 2001;103:196–200. [PubMed: 11208676]
6. Xiao Z, Guo W, Sun B, et al. Enhanced cytosolic Ca<sup>2+</sup> activation underlies a common defect of central domain cardiac ryanodine receptor mutations linked to arrhythmias. *J Biol Chem* 2016;291:24528–24537. [PubMed: 27733687]
7. Kimlicka L, Tung CC, Carlsson AC, Lobo PA, Yuchi Z, Van Petegem F. The cardiac ryanodine receptor N-terminal region contains an anion binding site that is targeted by disease mutations. *Structure* 2013;21:1440–1449. [PubMed: 23871484]

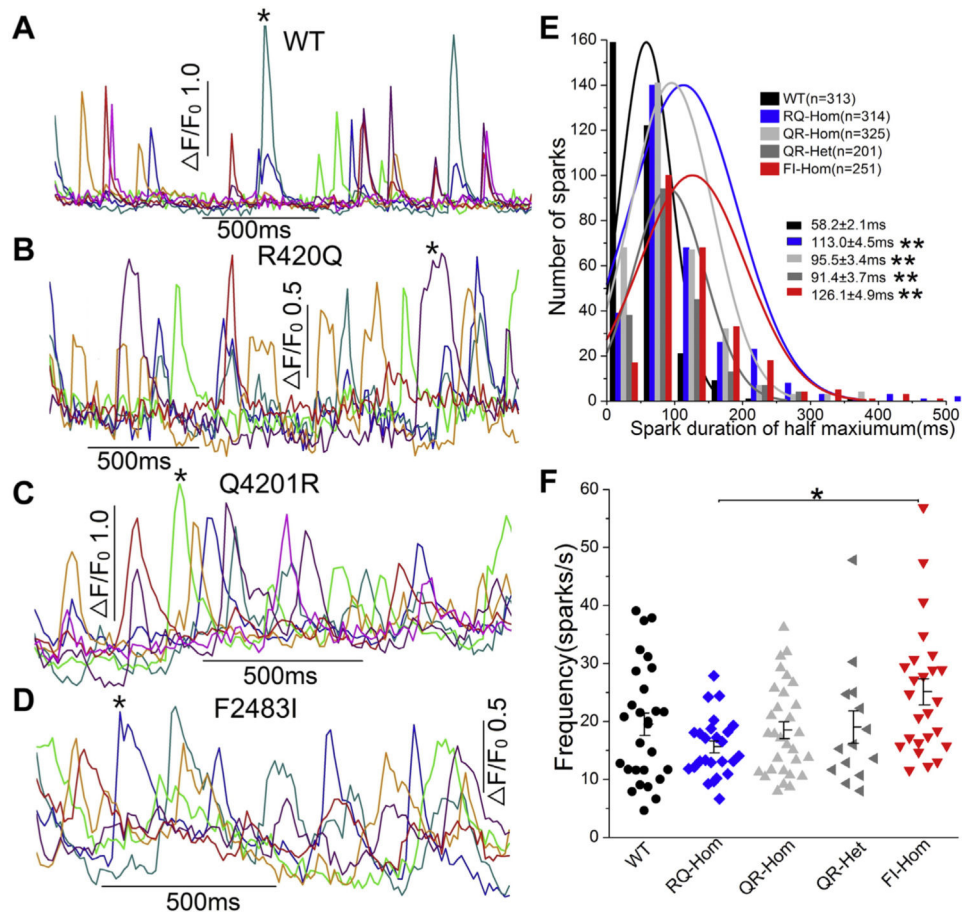
8. Jiang D, Xiao B, Yang D, et al. RyR2 mutations linked to ventricular tachycardia and sudden death reduce the threshold for store-overload-induced Ca<sup>2+</sup> release (SOICR). *Proc Natl Acad Sci USA* 2004;101:13062–13067. [PubMed: 15322274]
9. Liu N, Colombi B, Memmi M, et al. Arrhythmogenesis in catecholaminergic polymorphic ventricular tachycardia: insights from a RyR2 R4496C knock-in mouse model. *Circ Res* 2006;99:292–298. [PubMed: 16825580]
10. Marks AR, Priori S, Memmi M, Kontula K, Laitinen PJ. Involvement of the cardiac ryanodine receptor/calcium release channel in catecholaminergic polymorphic ventricular tachycardia. *J Cell Physiol* 2002;190:1–6. [PubMed: 11807805]
11. Wehrens XH, Lehnart SE, Huang F, et al. FKBP12.6 deficiency and defective calcium release channel (ryanodine receptor) function linked to exercise-induced sudden cardiac death. *Cell* 2003;113:829–840. [PubMed: 12837242]
12. Jiang D, Wang R, Xiao B, et al. Enhanced store overload-induced Ca<sup>2+</sup> release and channel sensitivity to luminal Ca<sup>2+</sup> activation are common defects of RyR2 mutations linked to ventricular tachycardia and sudden death. *Circ Res* 2005;97:1173–1181. [PubMed: 16239587]
13. Schlotthauer K, Bers DM. Sarcoplasmic reticulum Ca<sup>2+</sup> release causes myocyte depolarization: underlying mechanism and threshold for triggered action potentials. *Circ Res* 2000;87:774–780. [PubMed: 11055981]
14. Fujiwara K, Tanaka H, Mani H, Nakagami T, Takamatsu T. Burst emergence of intracellular Ca<sup>2+</sup> waves evokes arrhythmogenic oscillatory depolarization via the Na<sup>+</sup>-Ca<sup>2+</sup> exchanger: simultaneous confocal recording of membrane potential and intracellular Ca<sup>2+</sup> in the heart. *Circ Res* 2008;103:509–518. [PubMed: 18635824]
15. Takahashi K, Tanabe K, Ohnuki M, et al. Induction of pluripotent stem cells from adult human fibroblasts by defined factors. *Cell* 2007;131:861–872. [PubMed: 18035408]
16. Zhang XH, Haviland S, Wei H, et al. Ca<sup>2+</sup> signaling in human induced pluripotent stem cell-derived cardiomyocytes (iPS-CM) from normal and catecholaminergic polymorphic ventricular tachycardia (CPVT)-afflicted subjects. *Cell Calcium* 2013;54:57–70. [PubMed: 23684427]
17. Wei H, Zhang XH, Clift C, Yamaguchi N, Morad M. CRISPR/Cas9 gene editing of RyR2 in human stem cell-derived cardiomyocytes provides a novel approach in investigating dysfunctional Ca<sup>2+</sup> signaling. *Cell Calcium* 2018;73:104–111. [PubMed: 29730419]
18. Zhang XH, Saric T, Mehrjardi NZ, Hamad S, Morad M. Acid sensitive ion channels are expressed in human induced pluripotent stem cell-derived cardiomyocytes. *Stem Cells Dev* 2019;28:920–932. [PubMed: 31119982]
19. Hilliard FA, Steele DS, Laver D, et al. Flecainide inhibits arrhythmogenic Ca<sup>2+</sup> waves by open state block of ryanodine receptor Ca<sup>2+</sup> release channels and reduction of Ca<sup>2+</sup> spark mass. *J Mol Cell Cardiol* 2010;48:293–301. [PubMed: 19835880]
20. Lehnart SE, Terrenoire C, Reiken S, et al. Stabilization of cardiac ryanodine receptor prevents intracellular calcium leak and arrhythmias. *Proc Natl Acad Sci U S A* 2006;103:7906–7910. [PubMed: 16672364]
21. Jung CB, Moretti A, Mederos y Schnitzler M, et al. Dantrolene rescues arrhythmogenic RYR2 defect in a patient-specific stem cell model of catecholaminergic polymorphic ventricular tachycardia. *EMBO Mol Med* 2012;4:180–191. [PubMed: 22174035]
22. Kobayashi S, Yano M, Uchinoumi H, et al. Dantrolene, a therapeutic agent for malignant hyperthermia, inhibits catecholaminergic polymorphic ventricular tachycardia in a RyR2(R2474S/+) knock-in mouse model. *Circulation* 2010; 74:2579–2584.
23. Mallanna SK, Cayo MA, Twaroski K, Gundry RL, Duncan SA. Mapping the cell-surface *N*-glycoproteome of human hepatocytes reveals markers for selecting a homogeneous population of iPSC-derived hepatocytes. *Stem Cell Rep* 2016; 7:543–556.
24. Novak A, Barad L, Lorber A, et al. Functional abnormalities in iPSC-derived cardiomyocytes generated from CPVT1 and CPVT2 patients carrying ryanodine or calsequestrin mutations. *J Cell Mol Med* 2015;19:2006–2018. [PubMed: 26153920]
25. Penttinen K, Swan H, Vanninen S, et al. Antiarrhythmic effects of dantrolene in patients with catecholaminergic polymorphic ventricular tachycardia and replication of the responses using iPSC models. *PLoS One* 2015; 10:e0125366. [PubMed: 25955245]

26. Ran FA, Hsu PD, Wright J, Agarwala V, Scott DA, Zhang F. Genome engineering using the CRISPR-Cas9 system. *Nat Protoc* 2013;8:2281–2308. [PubMed: 24157548]
27. Zhang XH, Morad M.  $\text{Ca}^{2+}$  signaling of human pluripotent stem cells-derived cardiomyocytes as compared to adult mammalian cardiomyocytes. *Cell Calcium* 2020;90:102244. [PubMed: 32585508]
28. Paul-Pletzer K, Yamamoto T, Ikemoto N, et al. Probing a putative dantrolene-binding site on the cardiac ryanodine receptor. *Biochem J* 2005;387:905–909. [PubMed: 15656791]
29. Kobayashi S, Yano M, Suetomi T, et al. Dantrolene, a therapeutic agent for malignant hyperthermia, markedly improves the function of failing cardiomyocytes by stabilizing interdomain interactions within the ryanodine receptor. *J Am Coll Cardiol* 2009;53:1993–2005. [PubMed: 19460614]
30. Zima AV, Bovo E, Bers DM, Blatter LA.  $\text{Ca}^{2+}$  spark-dependent and -independent sarcoplasmic reticulum  $\text{Ca}^{2+}$  leak in normal and failing rabbit ventricular myocytes. *J Physiol* 2010;588:4743–4757. [PubMed: 20962003]
31. Polonen RP, Penttinen K, Swan H, Aalto-Setälä K. Antiarrhythmic effects of carvedilol and flecainide in cardiomyocytes derived from catecholaminergic polymorphic ventricular tachycardia patients. *Stem Cells Int* 2018;2018:9109503. [PubMed: 29760739]



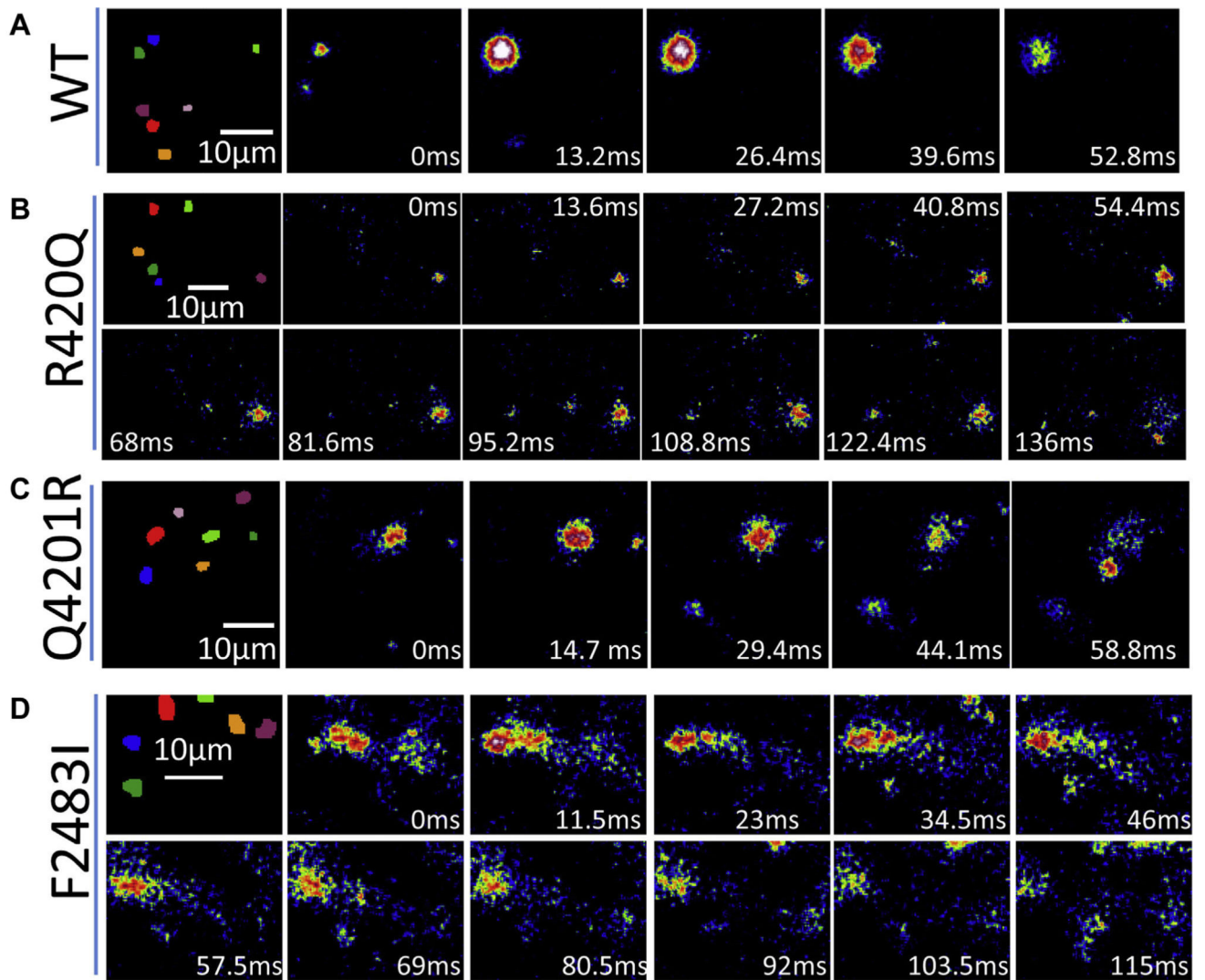
**Figure 1.**

Introduction of R420Q and Q4201R mutations into the ryanodine receptor 2 (*RYR2*) gene of hiPSCs. **A and B:** Sequencing of polymerase chain reaction (PCR) products show R420Q (CGG to CAG) and Q4201R (CAG to CGG) mutations. **C:** PCR analysis of the mutations. PCR products from homozygous mutants were completely digested into 2 fragments: 323 and 126 bp for R420Q and 340 and 141 bp for Q4201R. **D:** Quantification of RyR2 transcription levels in wild-type (WT) and mutant hiPSC-CMs.  $**P < .01$  vs WT. **E and F:** Western blot image and quantification of RyR2 protein levels in WT and 3 homozygous mutants. The F2483I homozygous clone was established in the previous study.<sup>17</sup>



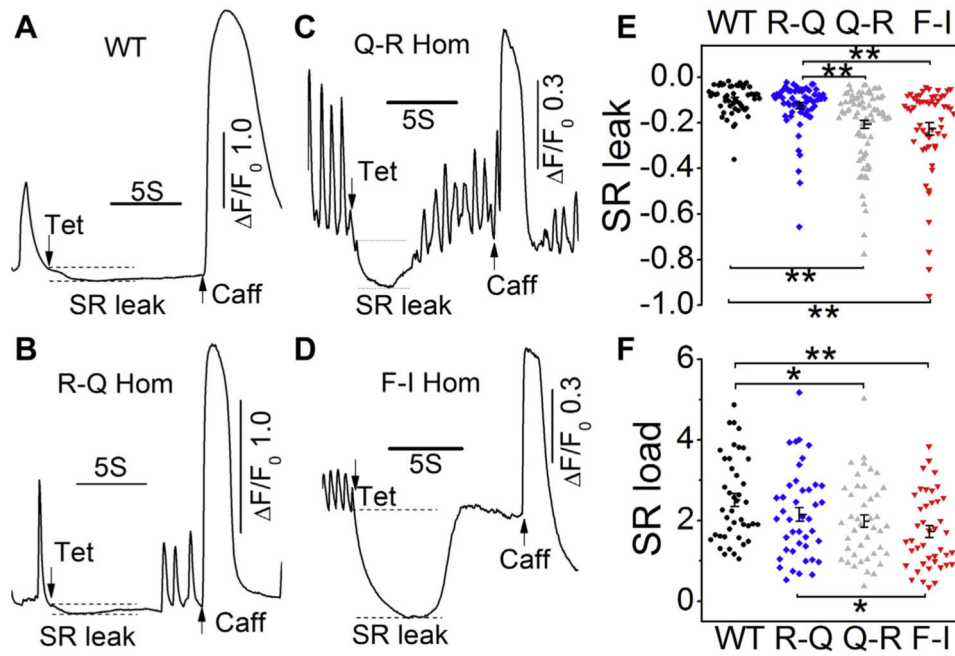
**Figure 2.**  $\text{Ca}^{2+}$  sparks recorded from wild-type (WT) and mutant hiPSC-CMs. **A–D:** Representative time courses of normalized  $\text{Ca}^{2+}$  sparks from the selected regions (*different colors*) in WT and 3 homozygous mutants. **E:** Histogram and distribution curves show the spark duration measured at half-maximum amplitude. \*\* $P < .01$  vs WT. Spark durations in F2483I and R420Q cells are significantly longer than those in Q4201R hiPSC-CMs ( $P < .01$ ). **F:** Spark frequency of WT and mutant cells. \* $P < .05$ , R420Q vs F2483I by 1-way analysis of variance. Part of the WT and F2483I-hom data are published previously.<sup>17</sup>



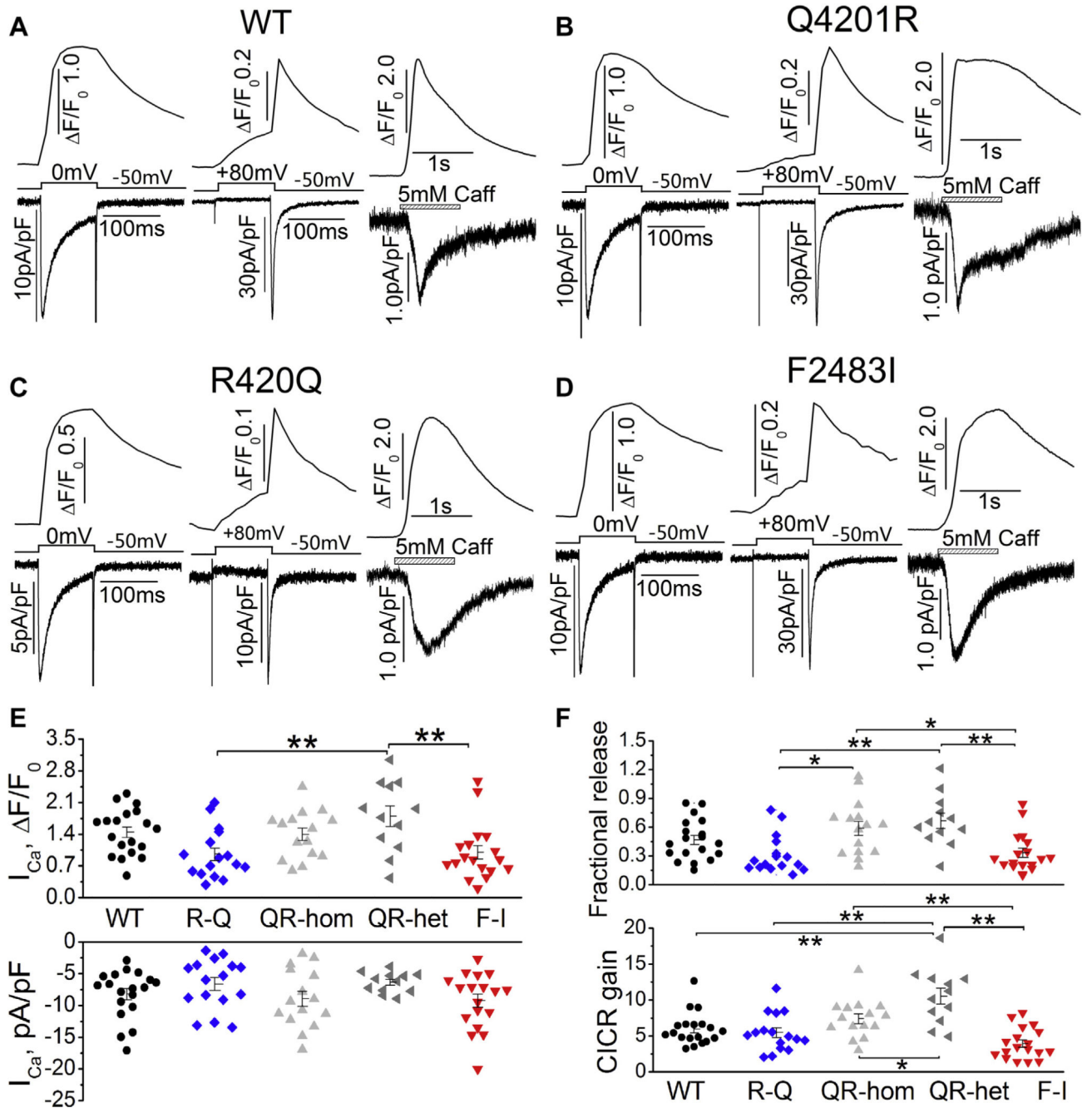


**Figure 3.** Total internal reflection fluorescence images show the evolution of the asterisk labeled sparks (Figure 2) from wild-type (A) and the 3 homozygous mutants (B–D). Note that R420Q and F2483I sparks are much longer.





**Figure 4.** SR Ca<sup>2+</sup> leak and load levels. **A–D:** Representative time courses of normalized Ca<sup>2+</sup> fluorescence changes after rapid exposure to 1 mM tetracaine followed by 5 mM caffeine in wild-type (WT) and 3 homozygous mutants. **E:** Scatter dot graph shows quantified sarcoplasmic reticulum (SR) leak levels, normalized to the SR store size. **F:** SR Ca<sup>2+</sup> content levels were determined by caffeine. \**P* < .05 and \*\**P* < .01 by 1-way analysis of variance. Part of the WT and F2483I-homozygous data are published previously.<sup>17</sup>

**Figure 5.**

L-type  $Ca^{2+}$  current ( $I_{Ca}$ ), fractional  $Ca^{2+}$  release, and calcium-induced calcium release (CICR) gain. **A–D**: Representative traces of  $I_{Ca}$  and  $I_{Ca}$ -induced  $Ca^{2+}$  release (*left panels*),  $I_{Ca}$  tail currents and their induced  $Ca^{2+}$  release (*middle panels*), and caffeine-induced  $Ca^{2+}$  release and  $I_{NCX}$  (*right panels*) from WT and 3 homozygous mutant hiPSC-CMs. **E**: Quantified  $I_{Ca}$  density (*bottom panel*) and  $I_{Ca}$ -induced  $Ca^{2+}$  release (*top panel*) in WT and mutant cells. **F**: Fractional  $Ca^{2+}$  release (*top panel*) and CICR gain (*bottom panel*) in each group. \* $P < .05$ , \*\* $P < .01$  by 1-way analysis of variance.

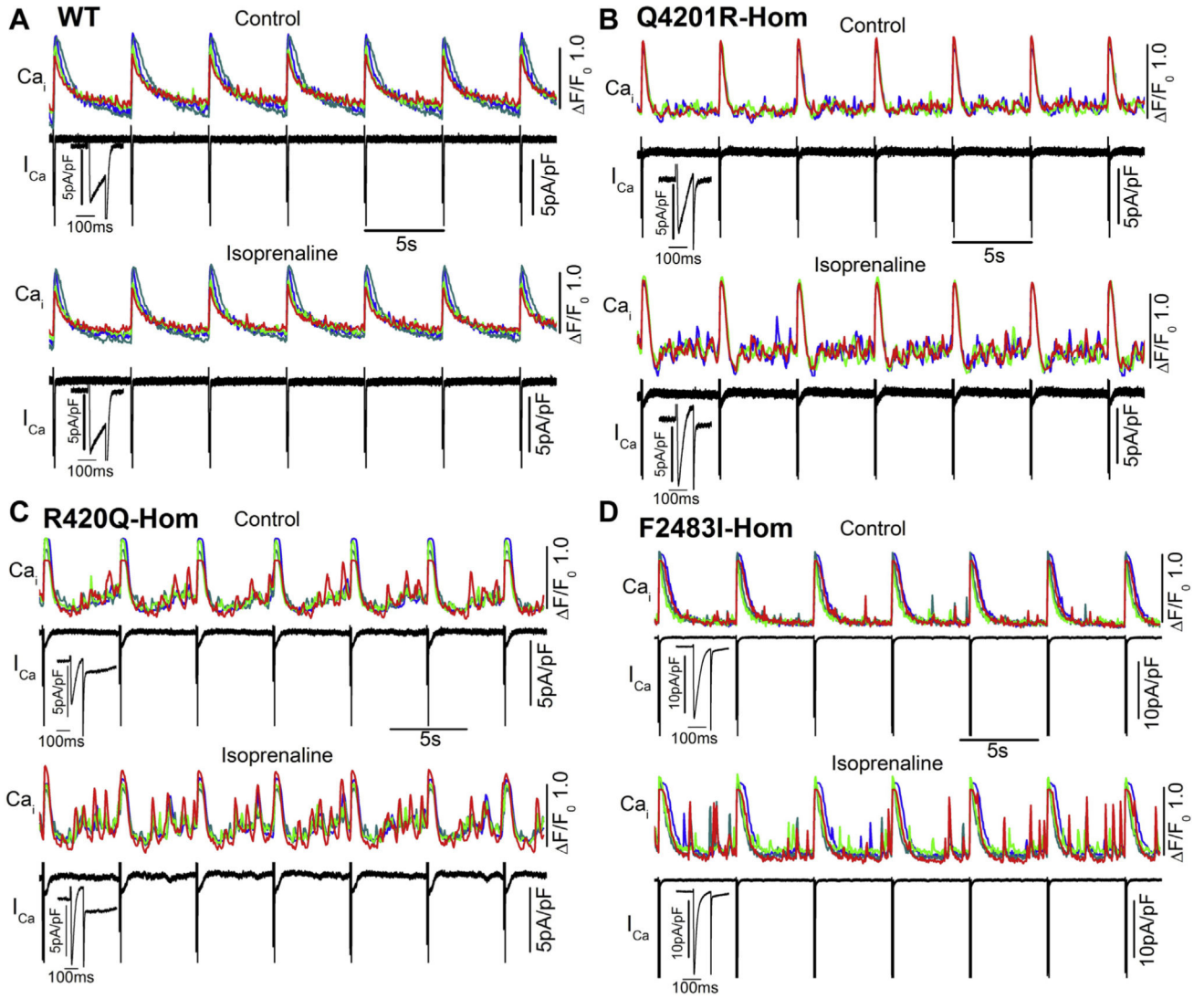


**Figure 6.**

Effect of adrenergic stimulation on L-type  $\text{Ca}^{2+}$  current ( $I_{\text{Ca}}$ ) and aberrant  $\text{Ca}^{2+}$  releases in wild-type (WT) and mutant hiPSC-CMs. Cells were stimulated by depolarization at 0.2 Hz (pulse train). **A–D**: The time course of cellular  $\text{Ca}^{2+}$  transients (colored) and 7  $I_{\text{Ca}}$  stimulation traces (black) before and after exposure to 500 nM isoprenaline in amphotericin B perforated patch-clamped WT and 3 homozygous mutant hiPSC-CMs. Enlarged  $I_{\text{Ca}}$  shows the first  $I_{\text{Ca}}$  trace from the pulse train.

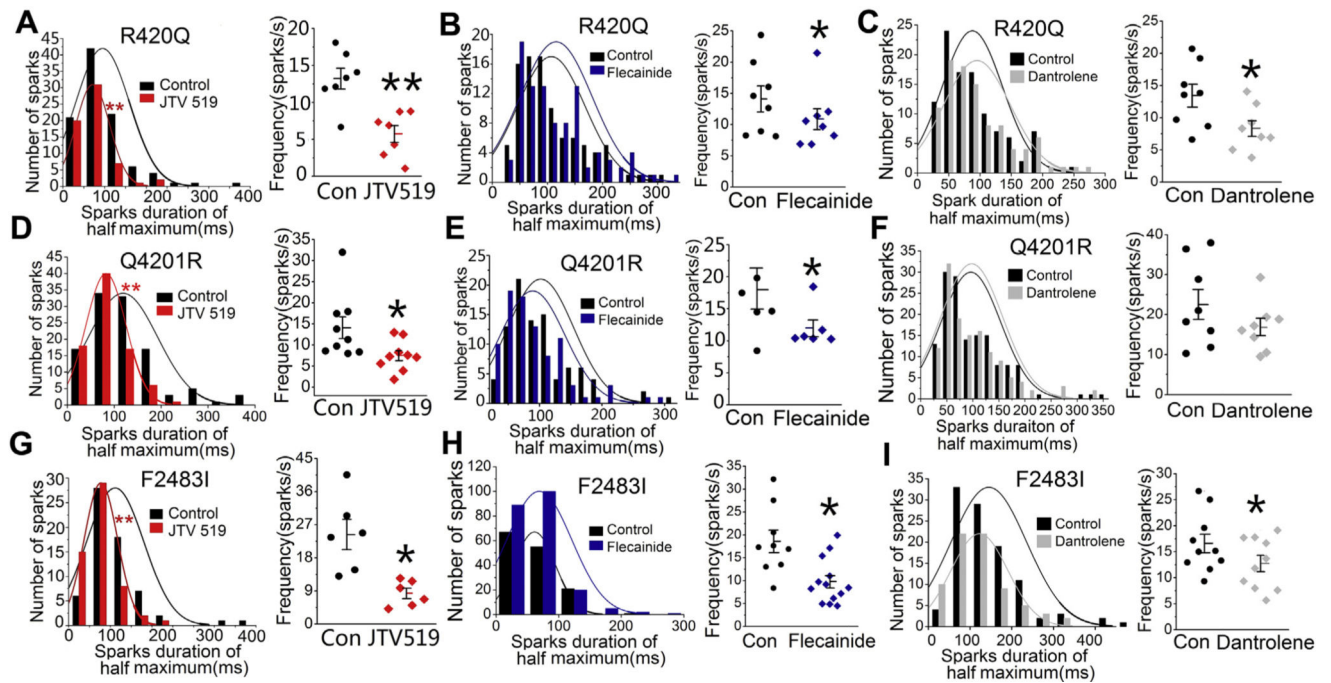


**Figure 7.**

Effects of JTV519, flecainide, and dantrolene on the  $\text{Ca}^{2+}$  sparks of 3 mutants. Effects of 2  $\mu\text{M}$  JTV519, 5  $\mu\text{M}$  flecainide, and 10  $\mu\text{M}$  dantrolene on the spark duration and frequency of R420Q (A–C), Q4201R (D–F), and F2483I (G–I) homozygous hiPSC-CMs. \* $P < .05$  and \*\* $P < .01$  vs control.



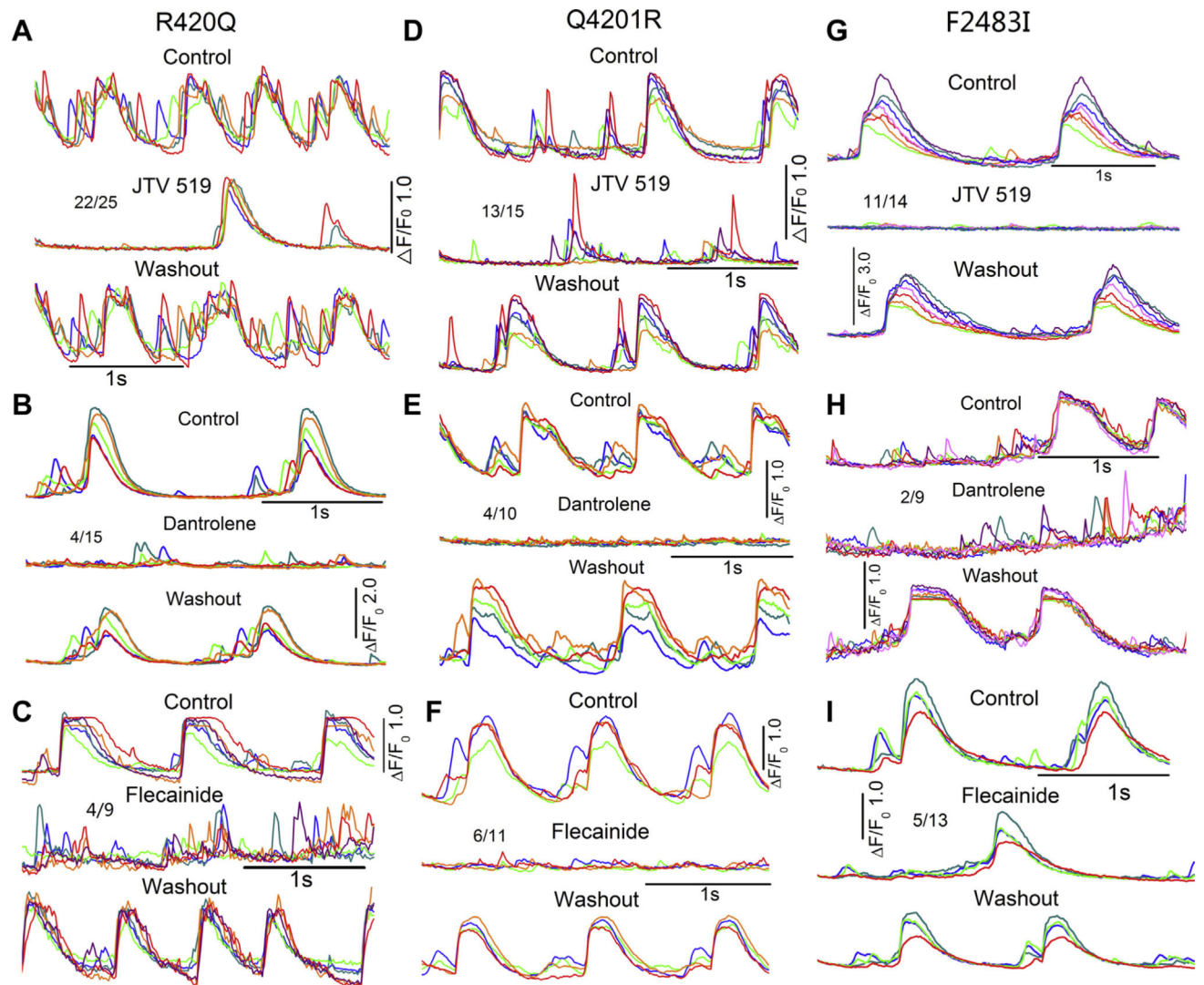


**Figure 8.** Effects of JTV519, dantrolene, and flecainide on the aberrant  $\text{Ca}^{2+}$  releases of mutant hiPSC-CMs. Representative traces of spontaneous  $\text{Ca}^{2+}$  transients with aberrant  $\text{Ca}^{2+}$  releases before and after exposure to and washout of 2  $\mu\text{M}$  JTV519, 10  $\mu\text{M}$  dantrolene, and 5  $\mu\text{M}$  flecainide on R420Q (A–C), Q4201R (D–F), and F2483I (G–I) homozygous hiPSC-CMs.